The salts of copper octafluoro- and hexadecafluorophthalocyanines containing $[Cu^{II}(F_8Pc)^{4-}]^{2-}$ dianions and $[CuF_{16}Pc]^-$ monoanions

Dmitri V. Konarev,*[a] Sergey I. Troyanov,[b] Alexey V. Kuzmin,[c] Yoshiaki Nakano,[d] Manabu Ishikawa,[d,e] Maxim A. Faraonov, [a] Salavat S. Khasanov,[c] Alexey L. Litvinov,[a] Akihiro Otsuka,[d] Hideki Yamochi,[d] Gunzi Saito[f] and Rimma N. Lyubovskaya[a]

[a]Institute of Problems of Chemical Physics RAS, Chernogolovka, Moscow region, 142432 Russia;

[b]Chemistry Department, Moscow State University, Leninskie Gory,119991 Moscow, Russia;

[c]Institute of Solid State Physics RAS, Chernogolovka, Moscow region, 142432 Russia;

[d]Department of Chemistry, Graduate School of Science, Kyoto University, Sakyo-ku, Kyoto, 606-8502, Japan;

[e]Agency for Health, Safety, and Environment, Kyoto University, Sakyo-ku, Kyoto 606-8501, Japan;

[f]Faculty of Agriculture, Meijo University, 1-501 Shiogamaguchi, Tempaku-ku, Nagoya 468-8502, Japan; Toyota Physical and Chemical Research Institute, 41-1, Yokomichi, Nagakute, Aichi 480-1192, Japan

Abstract–Crystalline anionic salts with copper octafluoro- and hexadecafluorophthalocyanines, $(Bu_4N^+)_2[Cu^{II}(F_8Pc)^{4-}]^{2-}\cdot 2C_6H_4Cl_2$ (**1**) and $(PPN^+)_3[CuF_{16}Pc]_3^{3-}\cdot 2C_6H_5CN$ (**2**), where PPN^+ is bis(triphenylphosphoranylidene)ammonium and Pc is phthalocyanine, have been obtained. The absence of noticeable absorption in the NIR range, and DFT calculations for **1**, indicate that both negative charges are mainly localized on the Pc ligand, and that the $[Cu^{II}(F_8Pc)^{4-}]^{2-}$ dianions are formed without reduction of Cu^{II}. The magnetic moment of 1.60 μ_B corresponds to the contribution of one $S = 1/2$ spin per dianion. The spin is localized on the Cu^{II} atom, which shows an EPR signal characteristic of Cu^{II}. Dianions are isolated in **1**, providing only weak magnetic coupling of spins with a Weiss temperature of –4 K. Salt **2** contains closely packed π-π stacks built of $[CuF_{16}Pc]^-$ anions of types I and II, and the interplanar distances are 3.187 and 3.275 Å. According to the DFT calculations, the $[CuF_{16}Pc]^-$ anions of types I and II can have different

charge distributions, with localization of an extra electron on the copper atoms to form diamagnetic $[Cu^{I}(F_{16}Pc)^{2-}]^{-}$ monoanions or delocalization of an extra electron on the $F_{16}Pc$ ligand to form $[Cu^{II}(F_{16}Pc)^{\bullet 3-}]^{\bullet -}$ having an S = 1/2 (Cu^{II}) + 1/2 ($F_{16}Pc^{\bullet 3-}$) spin state. In fact, at 300 K, the magnetic moment of **2** of 3.25 μ_B per formula unit is rather close to the contribution from two $[Cu^{II}(F_{16}Pc)^{\bullet 3-}]^{\bullet -}$ (calculated μ_{eff} is 3.46 μ_B). The Weiss temperature of –21.5 K indicates antiferromagnetic coupling of spins, which can be modeled by stronger intermolecular coupling between $(F_{16}Pc)^{\bullet 3-}$ with J_1/k_B = −23.5 K and weaker intramolecular coupling between Cu^{II} and $(F_{16}Pc)^{\bullet 3-}$ with J_2/k_B = −8.1 K. This interaction is realized in the $\{[Cu^{II}(F_{16}Pc)^{\bullet 3-}]^{\bullet -}\}_2$ dimers separated by diamagnetic $[Cu^{I}(F_{16}Pc)^{2-}]^{-}$ species. In spite of the stacking arrangement of phthalocyanine macrocycles in **2**, the inhomogeneous charge distribution and non-uniform distances between the macrocycles should suppress electrical conductivity.

KEYWORDS: copper (II) octafluoro- and hexadecafluorophthalocyanine, dianions, charge disproportionation, crystal structures, optical and magnetic properties

*Correspondence to: Dmitri V. Konarev, email: konarev@icp.ac.ru, FAX: +7 49652-21852.

Introduction

Metal phthalocyanines can possess promising conducting and magnetic properties in oxidized and reduced forms.[1–9] For example, electrochemical or chemical oxidation of metal phthalocyanines[1–2] or the $[M^{III}(CN)_2Pc]^{-}$ anions (M = Co, Fe, Pc is phthalocyanine)[3–5] yields compounds with a stacking arrangement of the Pc macrocycles and partial charge transfer. Some of these compounds show metallic conductivity down to liquid helium temperatures. Compounds with promising magnetic properties were obtained with manganese phthalocyanine or substituted phthalocyanine and tetracyanoethylene.[6–7]

Theoretical calculations show that reduced metal phthalocyanines can also manifest promising conducting properties, such as metallic conductivity or superconductivity.[8] A compound with ferrimagnetic ordering of spins was obtained through the reaction of iron (II) phthalocyanine with decamethylchromocene.[9] Several methods for the preparation of negatively

charged metal phthalocyanines as single crystals have been developed. For example, metal phthalocyanines are reduced by alkali metals in coordinating solvents,[10–11] Cp*Li (Cp*: pentamethylcyclopentadienyl),[12] or sodium fluorenone ketyl in the presence of organic cations.[13–19] Analysis of the crystal structures of these compounds shows that most of the metal phthalocyanine radical anions are packed in the crystals separately without noticeable π-π stacking.[10–18] The anions of iron (I) hexadecachlorophthalocyanine, due to the large size of the $[Fe^{I}(Cl_{16}Pc)^{2-}]^{-}$ anions, form stacks with effective π-π interactions between the macrocycles.[20–21] The stacks can be isolated with a uniform or non-uniform arrangement of the $Cl_{16}Pc$ macrocycles. Weak π-π interactions between phthalocyanines from the neighboring stacks also results in the formation of two-dimensional phthalocyanine layers.[21] The reduction of iron(II) hexadecachlorophthalocyanine is accompanied by the formation of iron (I) ions, retaining the Pc macrocycles in the dianionic state. As a result, relatively strong magnetic coupling between spins localized on the paramagnetic Fe(I) centers is observed.[20–21] However, high conductivity is not possible in these salts due to the fact that the $(Cl_{16}Pc)^{2-}$ macrocycles are still in the dianionic state and are diamagnetic.

In this study, we chose copper (II) octafluoro- and hexadecafluorophthalocyanines (CuF_8Pc and $CuF_{16}Pc$), whose reduction, in contrast to iron(II) hexadecachlorophthalocyanine, is centered on the Pc macrocycles. We obtained two salts: $(TBA^{+})_2[Cu^{II}(F_8Pc)^{4-}]^{2-}\cdot 2C_6H_4Cl_2$ (**1**) and $(PPN^{+})_3[Cu(F_{16}Pc)]_3^{3-}\cdot 2C_6H_5CN$ (**2**). Salt **1** contains isolated $[Cu^{II}(F_8Pc)^{4-}]^{2-}$ dianions. Closely packed π-π stacks of the $[Cu(F_{16}Pc)]^{-}$ monoanions are formed in 2, among which unusual variation in charge distribution is most probably realized. There is an internal degree of freedom in that one extra electron is accommodated on the copper atom forming the diamagnetic $[Cu^{I}(F_{16}Pc)^{2-}]^{-}$ anion or on the $F_{16}Pc$ ligand, forming a paramagnetic $[Cu^{II}(F_{16}Pc)^{\bullet 3-}]^{\bullet -}$ radical anion. We present and discuss for the first time the molecular structure, and the optical and magnetic properties of the compounds with the anions of fluorinated copper phthalocyanines.

EXPERIMENTAL

Materials

Sublimed grade copper (II) octafluorophthalocyanine [$Cu^{II}(F_8Pc)$] and copper (II) hexadecafluorophthalocyanine [$Cu^{II}(F_{16}Pc)$] (>98% purity) were purchased from TCI. Tetrabutylammonium bromide ($(Bu_4N)Br$, 99%) and bis(triphenylphosphoranylidene)ammonium ((PPN)Cl, 97%) were purchased from Aldrich. The reductant, sodium fluorenone ketyl, was obtained as described.[22] Solvents were purified under an argon atmosphere. The *o*-dichlorobenzene ($C_6H_4Cl_2$) was distilled over CaH_2 under reduced pressure, benzonitrile (C_6H_5CN) was distilled over sodium under reduced pressure and *n*-hexane was distilled over Na/benzophenone. Salts **1** and **2** were synthesized and stored in an MBraun 150B-G glove box with a controlled atmosphere containing less than 1 ppm of water and oxygen. Solvents were degassed and stored in the glove box. The KBr pellets used for IR and UV-visible-NIR analyses were prepared in the glove box. EPR and SQUID measurements were performed on polycrystalline samples of **1** and **2** sealed in 2 mm quartz tubes under 10^{-5} torr pressure.

General

UV-visible-NIR spectra were measured using KBr pellets on a Perkin Elmer Lambda 1050 spectrometer in the 250–2,500 nm range. FT-IR spectra were obtained using KBr pellets with a Perkin-Elmer Spectrum 400 spectrometer (400–7,800 cm^{-1}). A Quantum Design MPMS-XL SQUID magnetometer was used to measure the static magnetic susceptibility of **1** and **2** under a magnetic field of 100 mT, under cooling and heating conditions in the 300−1.9 K range. The sample-holder contribution and core temperature independent diamagnetic susceptibility (χ_d) were subtracted from the experimental values. The χ_d values were estimated from the extrapolation of the data in the high-temperature range, by fitting the data with the following expression: $\chi_M = C/(T - \Theta) + \chi_d$, where C is the Curie constant and Θ is the Weiss temperature. Effective magnetic moments (μ_{eff}) were calculated with the formula: $\mu_{eff} = (8\chi_M T)^{1/2}$.

Synthesis

Crystals of **1** and **2** were grown by a diffusion technique. The reaction mixture was filtered into a 50 mL glass tube 1.8 cm in diameter with a ground glass plug and then 30 mL of *n*-hexane was layered over the solution. Slow mixing of the solutions over 1–2 months resulted in precipitation of crystals. The solvent was then decanted from the crystals, and they were washed with *n*-hexane. The compositions of the obtained compounds were determined by X-ray diffraction analysis of a single crystal. Several crystals from one synthesis were found to consist of a single crystalline phase. Due to the high air sensitivity of **1** and **2**, elemental analysis could not be used to prove the composition.

$(Bu_4N)_2[Cu^{II}(F_8Pc)]\cdot 2C_6H_4Cl_2$ (**1**) was obtained via the reduction of $Cu^{II}(F_8Pc)$ (30 mg, 0.042 mmol), using an excess of sodium fluorenone ketyl (14 mg, 0.069 mmol) in the presence of an excess of $(Bu_4N)Br$ (30 mg, 0.092 mmol) in 16 ml of a 1:1 mixed solvent of *o*-dichlorobenzene and benzonitrile. The reaction was performed for two hours at 100°C. The resulting deep blue-violet solution was cooled down to room temperature and filtered into a tube for crystal growth. Black prisms were obtained in 68% yield.

$(PPN)_3[Cu^{II}(F_{16}Pc)]_3\cdot 2C_6H_5CN$ (**2**) was obtained via the reduction of $Cu^{II}F_{16}Pc$ (36 mg, 0.042 mmol), using an excess of sodium fluorenone ketyl (14 mg, 0.069 mmol) in the presence of one equivalent of (PPN)Cl (24 mg, 0.092 mmol) in 14 ml of benzonitrile. The reaction was performed for two hours at 100°C. The resulting deep blue-violet solution was cooled down to room temperature and filtered into a tube for crystal growth. Very thin black needles were obtained in 72% yield.

X-ray crystal structure determination

X-ray diffraction data for a crystal of **1** were collected on a Bruker Smart Apex II CCD diffractometer with graphite monochromated MoK_α radiation, using a Japan Thermal Engineering Co. cooling system DX-CS190LD. Raw data reduction to F^2 was carried out using Bruker SAINT.[23] The structures were solved by the direct method and refined by the full-matrix

least-squares method against F^2 using SHELX 2013.[24] Non-hydrogen atoms were refined in the anisotropic approximation. Positions of hydrogen were calculated geometrically. The structure contains disordered solvent $C_6H_4Cl_2$ molecules. One molecule is disordered between two orientations with the 0.403(4)/0.097(4) occupancies and another molecule has 0.5 occupancy. Both molecules are positioned in the inversion centers.

Table 1. X-ray diffraction data for salts **1** and **2**.

Compound	**1**	**2**
Structural formula	$(Bu_4N)_2[Cu(F_8Pc)]\cdot 2C_6H_4Cl_2$	$(PPN)_3[CuF_{16}Pc]_3\cdot 2C_6H_5CN$
Empirical formula	$C_{76}H_{88}Cl_4CuF_8N_{10}$	$C_{218}H_{100}Cu_3F_{48}N_{29}P_6$
M_r [g mol^{-1}]	1498.90	4413.70
Crystal color and shape,	Black block	Black needle
Size, mm×mm×mm	0.323×0.092×0.074	0.07×0.01×0.01
Crystal system	monoclinic	monoclinic
Space group	$P2_1/n$	$P2_1/n$
a, Å	8.5731(7)	22.847(1)
b, Å	25.247(2)	9.9281(3)
c, Å	16.6358(11)	40.385(1)
β,°	94.704(7)	97.718(5)
V, Å^3	3588.6(5)	9077.4(5)
Z	2	2
ρ_{calc} [g/cm^3]	1.387	1.615
μ [mm^{-1}]	0.525	0.520
F(000)	1566	4440
Absorption correction	none	none
T [K]	150.0(2)	100(2)
Max. 2Θ,°	58.68	69.48
Reflns measured	15088	120864
Unique reflns	7999	21841
Parameters, restraints	557, 288	1430, 0
Reflns [F_o>2σ(F_o)]	3380	20160
R_1 [F_o>2σ(F_o)]	0.1157	0.0418
wR_2 (all data)[a],	0.1964	0.1029
a	0.0241	0.0500
b	12.3467	11.0000
G.O.F	1.042	1.009
Restr. G.O.F.	1.029	1.009
CCDC number	1481219	1422989

(a) $w = 1/[\sigma^2(F_o^2) + (aP)^2 + bP]$, $P = [\mathrm{Max}(F_o^2,0) + 2F_c^2]/3$

X-ray diffraction data for a crystal of **2** were collected with a MAR225 CCD detector using synchrotron radiation at the BESSY storage ring, BL 14.2 (λ = 0.84344 Å), PSF of the Free University of Berlin, Germany. The structure was solved by the direct method and refined by the full-matrix least-squares method against F^2 using SHELX 2014.[24] Non-hydrogen atoms were

refined in the anisotropic approximation. Positions of hydrogen atoms were calculated geometrically. One of two independent PPN^+ cations contains a phenyl group disordered between two orientations with the 0.52/0.48(3) occupancies.

Computational details

Density functional theory (DFT) calculations were carried out by unrestricted methods based on the M11 functional.[25] For copper and the other atoms, cc-pVTZ-PP[26] and cc-pVDZ[27] basis sets were used, respectively. The calculations were performed using the "Int=SuperFineGrid" keyword. Full geometry optimization was done for D_{4h}-symmetric $[CuPc]^0$, $[Cu(F_8Pc)]^0$, and $[Cu(F_{16}Pc)]^0$. As for C_i-symmetric $[Cu(F_8Pc)]^{2-}$, only the coordinates of hydrogen atoms were geometry-optimized from the X-ray crystal structure data as the initial structure. As for the C_i-symmetric $[Cu(F_{16}Pc)]_3^{3-}$ trimer, where $CuF_{16}Pc$ molecules were stacked in a type II−type I−type II manner, the X-ray crystal structure data were used without geometry optimization. The stability of wave functions in the $[Cu(F_8Pc)]^{2-}$ and $[Cu(F_{16}Pc)]_3^{3-}$ trimers were checked by specifying the "Stable=Opt" keyword. The subsequent natural bond orbital (NBO) analysis was done by an NBO program.[28] All computations were performed with the Gaussian 09 program package.[29]

Results and Discussion

a. Synthesis

The preparation of single crystals of anionic salts of copper (II) octafluoro- and hexadecafluorophthalocyanines was possible only when high-purity starting compounds of sublimation grade (TCI, >98.0%) were used.

The presence of electron-withdrawing fluoro-substituents in these phthalocyanines makes them stronger acceptors[30] than $[Cu^{II}(Pc)^{2-}]^0$. The reduction of $[Cu^{II}(F_8Pc)^{2-}]^0$ by an excess of sodium fluorenone ketyl in the presence of excess TBA^+ cations was possible up to the dianionic state, whereas $[Cu^{II}(Pc)^{2-}]^0$ under the same conditions was reduced up to the monoanionic state only.[18] The reduction was carried out in a 1:1 mixture of *o*-dichlorobenzene and benzonitrile,

since the salt is poorly soluble in pure *o*-dichlorobenzene. $(TBA^+)_2[Cu^{II}(F_8Pc)^{4-}]^{2-}\cdot 2C_6H_4Cl_2$ (**1**) was formed as black blocks up to $0.4 \times 0.4 \times 0.6$ mm^3 in size. Salts of $[Cu^{II}(F_8Pc)^{4-}]^{2-}$ can also be obtained with the PPN^+ and Ph_3MeP^+ cations, but the crystals of these salts have the shape of extremely thin needles and their structures cannot be solved.

$[Cu^{II}(F_{16}Pc)^{2-}]^0$ was reduced selectively to the monoanionic state by a slight excess of fluorenone ketyl in the presence of a stoichiometric amount of the PPN^+ cations. The synthesis was carried out in pure benzonitrile, since reduced copper (II) hexadecafluorophthalocyanine is insoluble in *o*-dichlorobenzene. The crystals of $(PPN^+)_3[Cu(F_{16}Pc)]_3^{3-}\cdot 2C_6H_5CN$ (**2**) were formed as thin needles suitable for X-ray diffraction analysis using synchrotron radiation only. Similar salts can be obtained with the TBA^+ and Ph_3MeP^+ cations. However, we did not succeed in solving the crystal structures of these crystals. $[Cu^{II}(F_{16}Pc)^{2-}]^0$ can also be reduced to the dianionic state by an excess of the cations and reductant, but these salts are even less soluble in benzonitrile, and no crystals suitable for X-ray diffraction analysis could be obtained in this case.

b. Optical properties.

The starting $[Cu^{II}(F_8Pc)^{2-}]^0$ and $[Cu^{II}(F_{16}Pc)^{2-}]^0$ show similar spectra in the UV-visible-NIR range, manifesting Soret bands at 30 cm^{-1}, 120 cm^{-1}, and 29,500 cm^{-1} (332 nm and 339 nm), and split Q-bands at 16,233 cm^{-1}, 14,900 cm^{-1}, and 13,717 cm^{-1} (616 nm, 671 nm, and 729 nm) and 16,077 cm^{-1}, 14,100 cm^{-1}, and 12,674 cm^{-1} (622, 709, and 789 nm), respectively (Fig. 1). Both phthalocyanines also show weak bands in the NIR range at 9,260 cm^{-1} (1,080 nm) and 8,800 cm^{-1} (1137 nm), respectively. It is seen that all bands in the spectrum of $[Cu^{II}(F_{16}Pc)^{2-}]^0$ are noticeably red-shifted in comparison with those in the spectrum of $[Cu^{II}(F_8Pc)^{2-}]^0$. Previously, we showed that the reduction centered on the Pc ligand of $Cu^{II}Pc$ is accompanied by the appearance of a new intense band in the NIR range at 10,480 cm^{-1} (954 nm), with a noticeable blue shift of both the Soret and Q-bands.[18] The presence of two TBA^+ cations per one $Cu^{II}F_8Pc$ in **1** justifies its dianionic state. Salt **1** manifests absorption bands at 31,350 cm^{-1}, 16,950 cm^{-1},

and 15,015 (shoulder) cm^{-1} (319, 590 nm and 666 nm) and a weak band at 9,870 cm^{-1} (1,013 nm) (Fig. 1a). Since the absorption band in the spectrum of **1** in the NIR range is weak, it can be concluded that two extra electrons in the dianion are accommodated on the F_8Pc macrocycle to form closed-shell $(F_8Pc)^{4-}$ tetraanions in $[Cu^{II}(F_8Pc)^{4-}]^{2-}$. The presence of eight electron-withdrawing fluoro-substituents in $Cu^{II}F_8Pc$ can facilitate the accommodation of both electrons of the dianion on the Pc macrocycle. Additionally, the reduction of Cu^{II} is not supported by optical spectra, since the $[Cu^{I}(F_8Pc)^{\bullet 3-}]^{\bullet -}$ species should have an intense absorption band in the NIR range similarly to $[Cu^{II}(Pc)^{\bullet 3-}]^{\bullet -}$ [18] but only one weak band at 9,870 cm^{-1} (1,013 nm) can be associated with these species. Both Soret and Q-bands are noticeably blue-shifted in the spectrum of **1** in comparison with the spectrum of neutral $[Cu^{II}(F_8Pc)^{2-}]^0$ (Fig. 1a). The spectrum of **1** is similar to those of reduced metal phthalocyanines containing Pc^{4-} tetraanions, such as $[Nb^{IV}O(Pc)^{4-}]^{2-}$, $[Ge^{IV}(Pc)^{4-}]^0$, $[Zr^{IV}(Pc)^{4-}]^0$, and $[Sn^{II}(Pc)^{4-}]$.[31–33]

The ratio of the PPN^+ cations and $Cu^{II}(F_{16}Pc)$ in **2** is 1:1, indicating that the formal charge on $Cu^{II}(F_{16}Pc)$ is −1. This manifests intense absorption bands at 30,864 cm^{-1} and 17,513 cm^{-1} (324

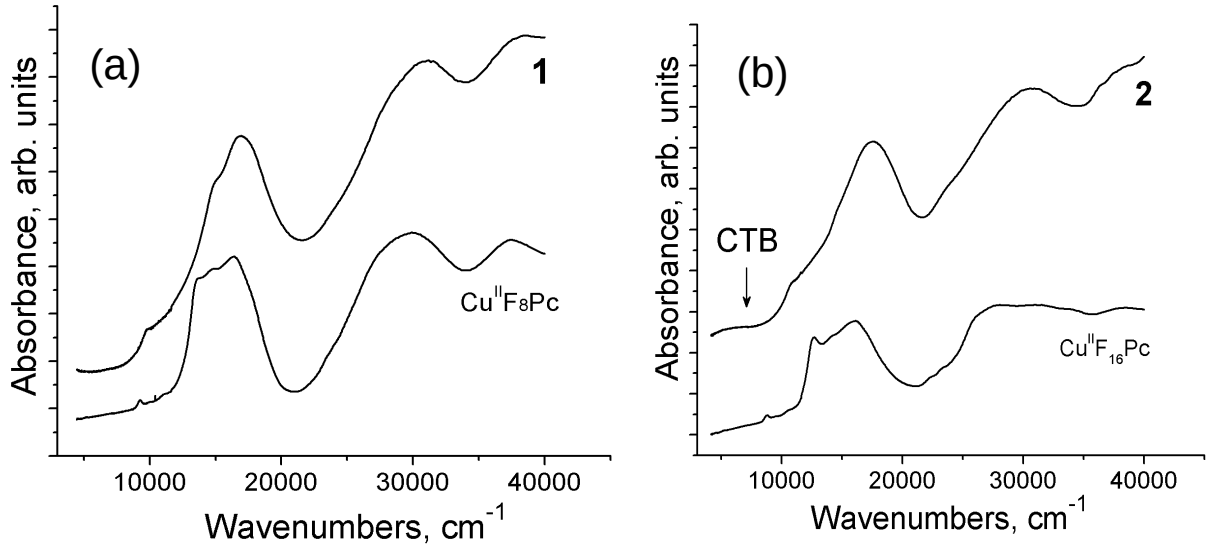

Figure 1. Spectra of: (a) starting $[Cu^{II}(F_8Pc)^{2-}]^0$ and salt **1**; (b) starting $[Cu^{II}(F_{16}Pc)^{2-}]^0$ and salt **2** in the UV-visible-NIR range measured in KBr pellets prepared in anaerobic conditions. Arrow marks charge transfer band (CTB).

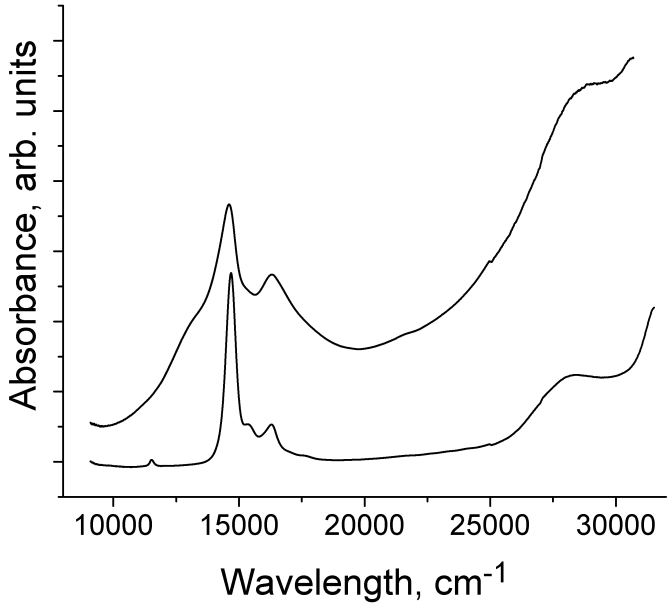

Figure 2. Spectra of starting $[Cu^{II}(F_{16}Pc)^{2-}]^0$ and monoreduced $[Cu^{II}(F_{16}Pc)^{\bullet 3-}]^{\bullet -}$ species in benzonitrile solution. Monoreduced species were obtained by the reduction of $[Cu^{II}(F_{16}Pc)^{2-}]^0$ by sodium fluorenone ketyl in the presence of one equivalent of (PPN)Cl.

and 571 nm), and a weaker band is manifested as a shoulder in the NIR range at 10,965 cm^{-1} (912 nm) (Fig. 1b). The appearance of the latter band indicates the presence of $[Cu^{II}(F_{16}Pc)^{\bullet 3-}]^{\bullet -}$ in **2**. It is also seen that both Soret and Q-bands are manifested as single bands and are strongly blue-shifted in **2** relative to those in the spectrum of neutral $[Cu^{II}(F_{16}Pc)^{2-}]^0$. Therefore, blue shifts of both Soret and Q-bands are characteristic of reduced fluorinated copper (II) phthalocyanines. Similar blue shifts of these bands were found previously for the $(Bu_4N^+)_2[Cu^{II}(Pc)^{\bullet 3-}]^{\bullet -}(Br^-)$ salt and other salts containing $Pc^{\bullet 3-}$.[18] Solution spectra of $[Cu^{II}(F_{16}Pc)^{2-}]^0$ and monoreduced $[Cu^{II}(F_{16}Pc)^{\bullet 3-}]^{\bullet -}$ are shown in Fig. 2. $[Cu^{II}(F_{16}Pc)^{2-}]^0$ manifests a triple Q-band at 14,723 (680 nm), 15,427 (648 nm), and 16,323 cm^{-1} (612 nm), and a Soret band at 28,464 cm^{-1} (351 nm). Upon reduction, these bands were broadened, with slight shifts to lower energies and the low-energy shoulder appeared at 12,950 cm^{-1} (772 nm) (Fig. 2).

c. Crystal structures

The crystal structure of **1** was solved, with a relatively high R_1 value of 0.1134. The reason for this is the presence of strongly disordered solvent molecules. Nevertheless, the geometry of Cu(F_8Pc) in **1** was solved with reasonable accuracy. The structure of **1** is shown in Fig. 3. The centrosymmetric $[Cu^{II}(F_8Pc)^{4-}]^{2-}$ dianions are completely isolated and alternate with the Bu_4N^+ cations along the *a* axis. The average Cu–N(pyrrole) bond length in **1** is 1.961(5) Å. There are two types of C–N bonds in the Pc macrocycle with imine and pyrrole nitrogen atoms. There are four shorter (1.283(8) Å) and four longer (1.374(8) Å) C-N (imine) bonds. They are located in such a way that they belong to two oppositely located isoindole units. The alternation of the C–N (imine) bonds can be explained by partial disruption of aromaticity of the Pc macrocycle due to the formation of an antiaromatic 20 π-electron system in the $(F_8Pc)^{4-}$ tetraanion. Similar alternation of the C–N (imine) bonds was found in $[Cu^{II}(Pc)^{\bullet 3-}]^{\bullet -}$ and other salts containing $Pc^{\bullet 3-}$.[18] Alternation of the C–N (pyrrole) bonds is also observed in **1**, with average values of 1.364(8) and 1.456(8) Å for shorter and longer bonds. It should be noted that no alternation of these bonds was found in $[Cu^{II}(Pc)^{2-}]^0$ [34] and $[Cu^{II}(Pc)^{\bullet 3-}]^{\bullet -}$ [18]. The average C–F bond length in **1** was 1.381(7) Å.

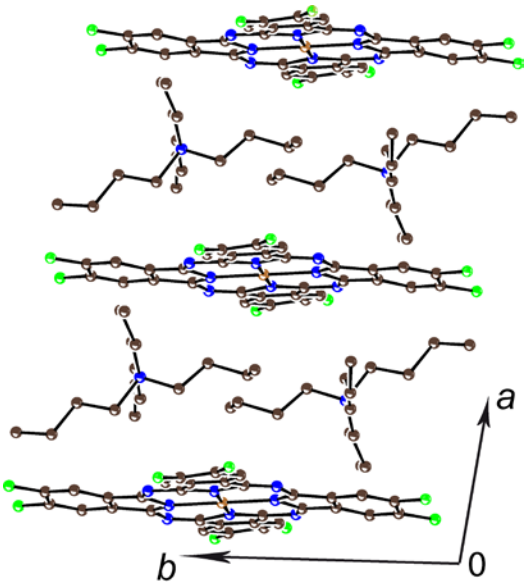

Figure 3. Crystal structure of **1**; the $[Cu^{II}(F_8Pc)^{4-}]^{2-}$ dianions alternating with the Bu_4N^+ cations along the *a* axis are shown.

There are two unique $Cu(F_{16}Pc)^-$ anions in **2** on a center of inversion and in a general position (marked as I and II, respectively, in Fig. 4a). These anions form closely packed π-π stacks arranged along the *b* axis and isolated by the PPN^+ cations (Fig. 4b). Interplanar distances between phthalocyanines are not uniform in the stacks, with shorter (3.187 Å) and longer (3.275 Å) interplanar distances between the anions of type I and II and between the anions of type II, respectively. The appearance of two crystallographically independent $[Cu(F_{16}Pc)]^-$ anions in **2** with different interplanar distances can be explained by different charge distributions in the anions of type I and II (see theoretical part). The anions of type I and II have average lengths of Cu–N (pyrrole) and C–F bonds of 1.9495(15) and 1.344(2) Å (I) and 1.9542(15) and 1.345(2) Å (II). In both cases, no alternation of the C–N (imine) and C–N (pyrrole) bonds has been found, and these are close to 1.326–1.327(2) Å and 1.376–1.378(2) Å, respectively. The Cu atoms are located exactly in the 24-atom Pc plane in the anions of type I and deviate by 0.043 Å from the 24-atom plane for the anions of type II. The anions of type II have essentially stronger deviation from planarity than the anions of type I. The C–F bonds are essentially longer by about 0.037–0.038 Å in **1** than those in **2**. This can be explained by the accommodation of an extra electron in

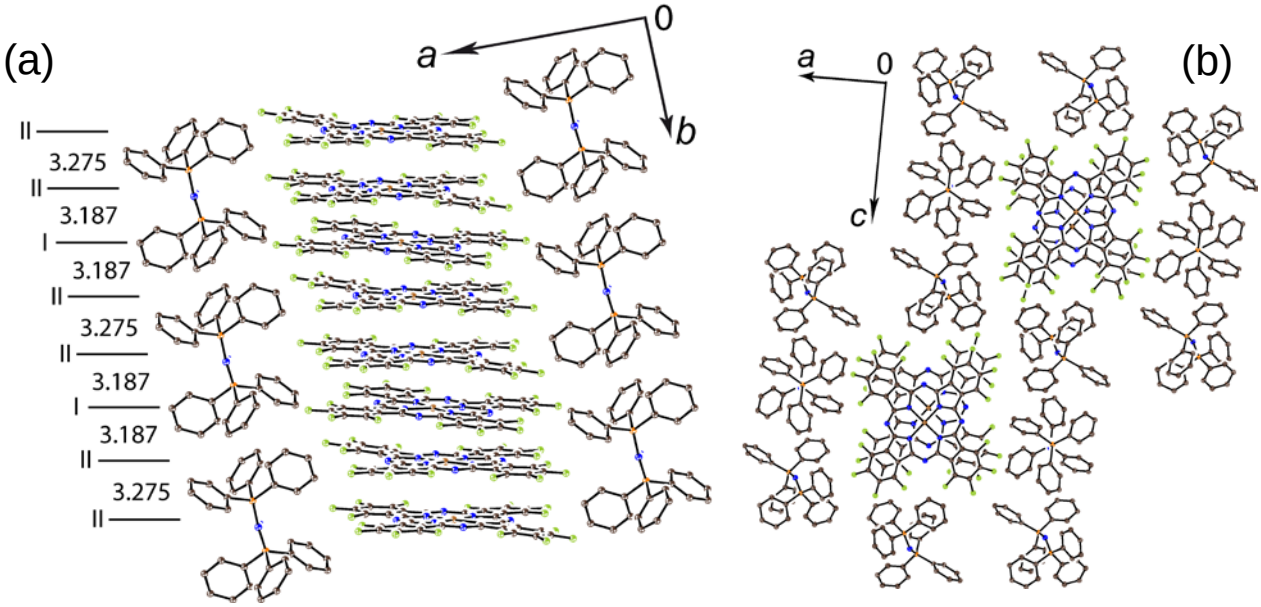

Figure 4. Crystal structure of **2**, view on (a) and along (b) the π-stacking columns from the $CuF_{16}Pc$ anions surrounded by the PPN^+ cations. Solvent molecules are not shown for clarity.

the lowest unoccupied molecular orbital (LUMO), with the antibonding character of the C–F bond in $[Cu^{II}(F_8Pc)^{2-}]^0$ and $[Cu^{II}(F_{16}Pc)^{2-}]^0$. The increase in the occupation number of the LUMO shortens the C–F bonds.

Overlap integrals between the $[Cu(F_{16}Pc)]^-$ anions in the π-π stacks of **2** were calculated by an extended Hückel method,[35] using single crystal X-ray diffraction data. Since there are two different interplanar distances of 3.187 and 3.275 Å, two overlap integrals, s1 and s2, respectively, were obtained (Fig. 5a), whereas the type of overlapping between phthalocyanines for integrals s1 and s2 is shown in Figs 5b and 5c. Integral s1 (between the anions of type I and II) has values of 0.0014 and 0.0052 for the LUMO-LUMO and HOMO-HOMO overlapping, respectively, whereas integral s2 between the anions of type II is 0.0040 and 0.0001 for the LUMO-LUMO and HOMO-HOMO overlapping, respectively. This is in agreement with a shorter interplanar distance between the anions of type I and II (Fig. 4a). The overlap integral s1 in **2** is comparable with those (0.0049–0.0100) in the π-stacking compounds of $[Fe^{I}(Cl_{16}Pc)^{2-}]^-$ [20–21] and conducting salts with the oxidized $[M^{III}(CN)_2(Pc)^{2-}]^-$ anions (M = Co, Fe). [4, 5, 36–38]

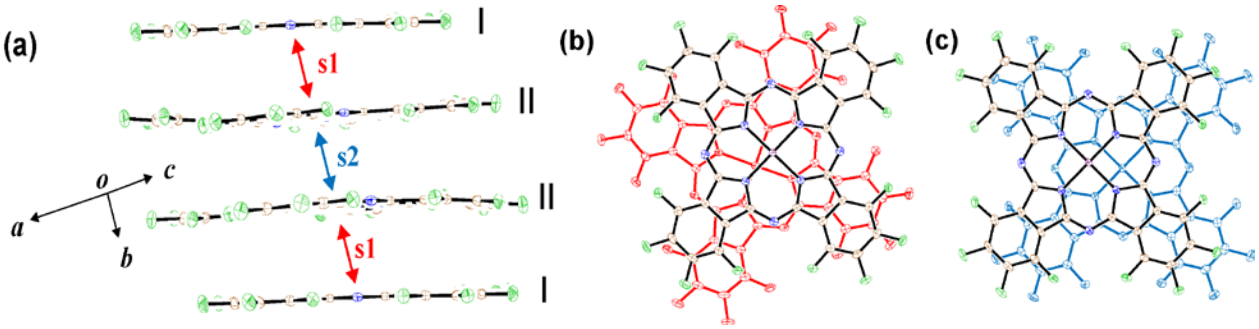

Figure 5. (a) The stacking column structure of salt **2** (a) and type of overlapping for s1 (b) and s2 (c). One of the two molecules in (b) and (c) is colored red and blue, respectively.

d. Theoretical analysis

To examine the electronic structure of the $[Cu(F_8Pc)]^{2-}$ dianion, theoretical analysis based on density functional theory (DFT) was performed. The total energy, the $<S^2>$ value, and the Mulliken and natural charges and spins are summarized along with the related materials in Tables S2 and S3. The energy diagram for the frontier Kohn-Sham orbitals in the ^2A_g state of $[Cu(F_8Pc)]^{2-}$ is shown in Fig. 6a. The highest occupied (HO) orbital stems from the doubly degenerate lowest unoccupied (LU) orbital in the $^2B_{1g}$ state of $[Cu^{II}(F_8Pc)^{2-}]^0$ (Fig. S4). Therefore, the F_8Pc ligand in $[Cu(F_8Pc)]^{2-}$ can be formally regarded as a closed-shell F_8Pc^{4-} tetraanion. As shown in Figs S4 and S6, the electrostatic potential map for $[CuF_8Pc]^{2-}$ is quite asymmetric as compared with that of $[Cu^{II}(F_8Pc)^{2-}]^0$, where the isoindole moieties over which the HO orbital spreads are more negatively charged than the other ones. Comparing the charge distribution of $[Cu(F_8Pc)^{4-}]^{2-}$ with that of $[Cu^{II}(F_8Pc)^{2-}]^0$ (Table S3), it should be concluded that

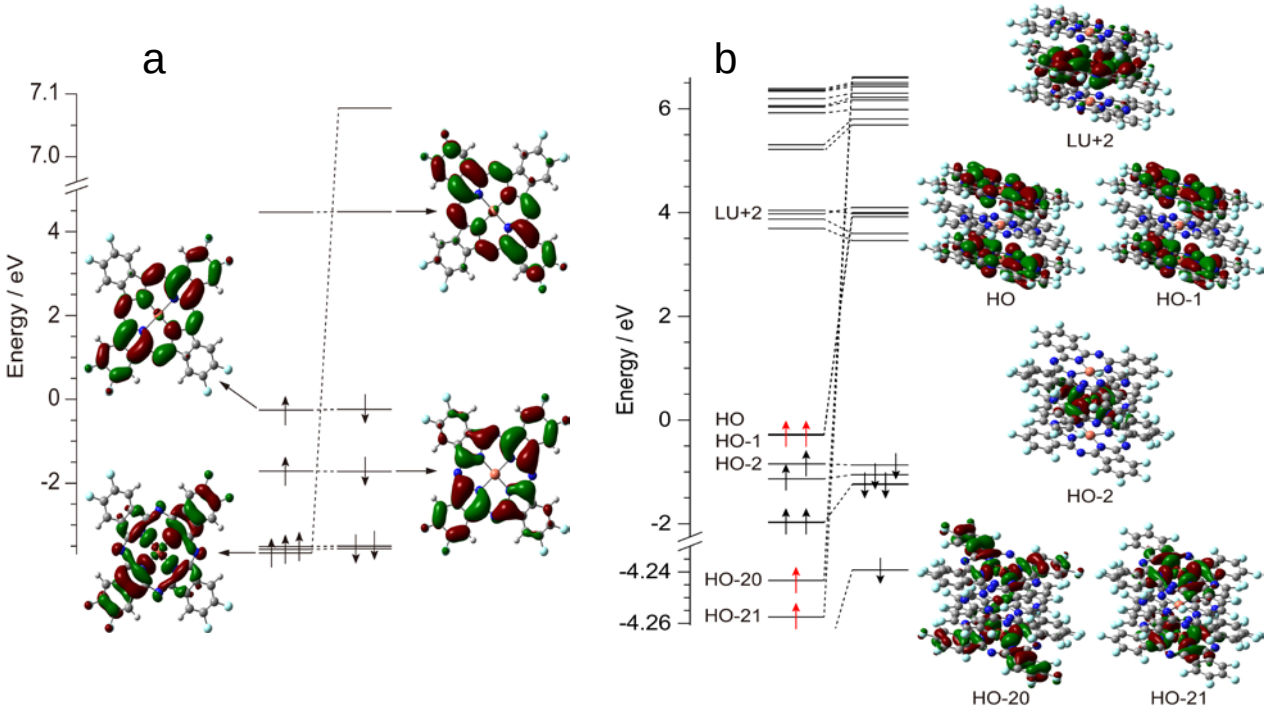

Figure 6. Energy diagram for the frontier Kohn-Sham orbitals in (a) ^2A_g state of $[Cu^{II}(F_8Pc)^{4-}]^{2-}$ and (b) ^5A_g state of C_i-symmetric $[Cu(F_{16}Pc)]_3^{3-}$ trimer. Selected α orbitals are shown and α spins in singly occupied orbitals are indicated by red arrows.

the charge on copper is nearly the same, but F_8Pc in $[Cu(F_8Pc)^{4-}]^{2-}$ is more negatively charged by about two electrons compared with that in $[Cu^{II}(F_8Pc)^{2-}]^0$. On the other hand, the spin distribution is nearly identical (Table S3 and Figs S4 and S6). The present theoretical analysis supports the scenario that two extra electrons are accommodated in the LU orbital of $[Cu^{II}(F_8Pc)^{2-}]^0$ to afford the closed-shell F_8Pc^{4-} tetraanion on the formal charge basis.

Then, the electronic structures on the quintet, triplet, and singlet states of the $[Cu(F_{16}Pc)]_3^{3-}$ trimer, where the $CuF_{16}Pc$ molecules are stacked in a type II − type I− type II manner, were also analyzed at the same level of theory. The total energy, the $<S^2>$ value, and the Mulliken and natural charges and spins are summarized along with related materials in Tables S2 and S3. The quintet state is the most stable. The energy diagram for the frontier Kohn-Sham orbitals in the ^5A_g state of the $[CuF_{16}Pc]_3^{3-}$ trimer is shown in Fig. 6b. Singly occupied orbitals spread over the type-II $CuF_{16}Pc$ molecule, where the α-HO and α-(HO−1) orbitals stem from the LUMO of $[Cu(F_{16}Pc)]^0$, and the α-(HO−20), and α-(HO−21) orbitals are composed of copper 3*d* orbitals.

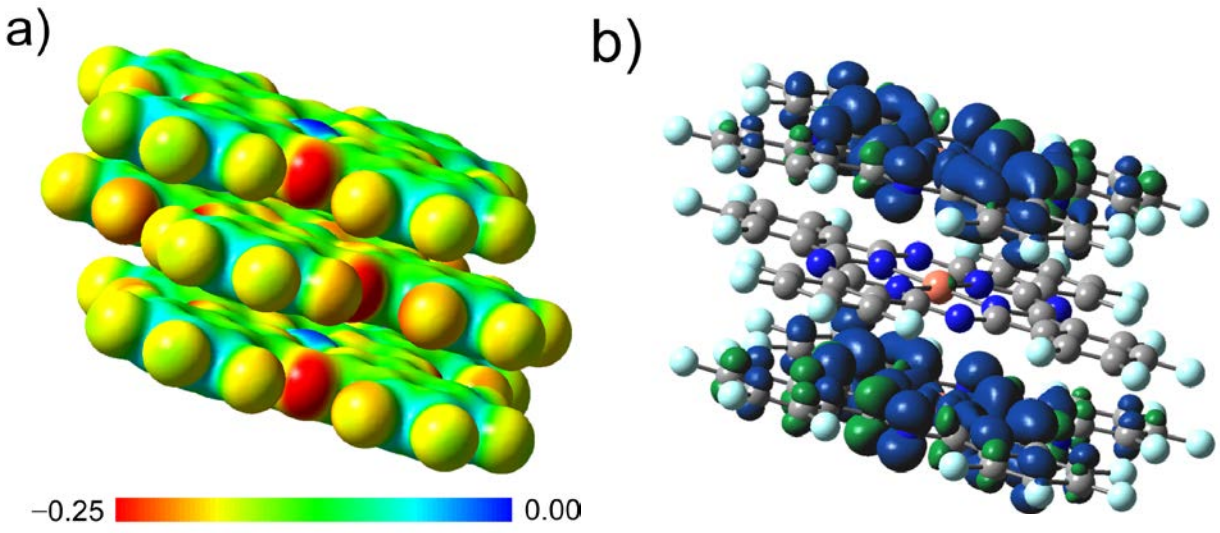

Figure 7. (a) Electrostatic potential map on 0.02 electrons/au^3 of electron density surface, and (b) spin density distribution, in which the isosurface value is 0.0016 electrons/au^3 and the isosurfaces in blue and green denote positive and negative spin density, in the ^5A_g state of the C_i-symmetric $[Cu(F_{16}Pc)]_3^{3-}$ trimer calculated at the UM11/cc-pVTZ-PP/cc-pVDZ level of theory.

Therefore, the type-II $CuF_{16}Pc$ molecule is a two-spin system consisting of a central copper and a $F_{16}Pc$ π-radical anion. On the other hand, α-(LU+2) and α-(HO−2) orbitals, which spread over the central type-I $CuF_{16}Pc$ molecule, stem from the LU orbital of $[Cu(F_{16}Pc)^{2-}]^0$ and are composed of copper 3*d* orbitals. Therefore, the type-I $CuF_{16}Pc$ molecule is not magnetic because the orbitals of both copper and $F_{16}Pc$ are closed-shell. As shown in Fig. 7a, the electrostatic potential map in the $[Cu(F_{16}Pc)]_3^{3-}$ trimer is inhomogeneous, especially on the central copper atoms. Comparing the charge distribution of $[Cu^{II}(F_{16}Pc)^{2-}]^0$ (Table S3) with that of the type-II $CuF_{16}Pc$ molecule, it should be concluded that the charge on copper is nearly the same, but the $F_{16}Pc$ macrocycle is more negatively charged by about one electron. However, as for the type-I $CuF_{16}Pc$ molecule, the charge on copper is apparently smaller than those on $[Cu^{II}(F_{16}Pc)^{2-}]^0$ and the type-II $CuF_{16}Pc$ molecules. Focusing on the natural electron configuration of the copper 3*d* orbital, only the type-I $CuF_{16}Pc$ molecule has $3d^{9.80}$, whereas the type-II $CuF_{16}Pc$ molecule has $3d^{9.25}$ (Table S3), indicating that the electron configurations of copper in the type I and II $CuF_{16}Pc$ molecules are Cu^+ ($3d^{10}$) and Cu^{2+} ($3d^9$), respectively. Therefore, the present theoretical analysis suggests that the charge distribution in the $[Cu(F_{16}Pc)]^-$ anions within the stacks is of a $[Cu^{II}(F_{16}Pc)^{\bullet 3-}]^{\bullet -}\cdots[Cu^{I}(F_{16}Pc)^{2-}]^{-}\cdots[Cu^{II}(F_{16}Pc)^{\bullet 3-}]^{\bullet -}\cdot$manner along the type II − type I − type II stack, although all the $CuF_{16}Pc$ molecules have the same molecular charge of −1.

Previously, charge disproportionation was found within the π-stacks from the iron (I) hexadecachlorophthalocyanine anions. However, since the reduction of $Fe^{II}Cl_{16}Pc$ is centered on the iron atoms, differently charged Fe atoms are formed within the stacks due to charge disproportionation.[20] The phenomena of different charge distributions for one type of phthalocyanine anion was found for the first time. This may be attributable to an internal degree of freedom, where one extra electron is accommodated in the copper atoms or on the $F_{16}Pc$ ligand. The difference in the molecular shapes of the $[Cu(F_{16}Pc)]^-$ anions of type I and II is induced by the effect of vibronic and/or electron-electron interactions. Since the overlap integrals

are relatively small in **2**, such interactions are considered to be dominant. While the conducting path is formed by the $F_{16}Pc$ stacking column, the inhomogeneous charge distribution in the columns should suppress electrical conductivity. Calculations with larger clusters (e.g., $[Cu(F_{16}Pc)]_6^{6-}$ hexamer) or with periodic boundary conditions are also planned, and the results will be published separately.

e. Magnetic properties

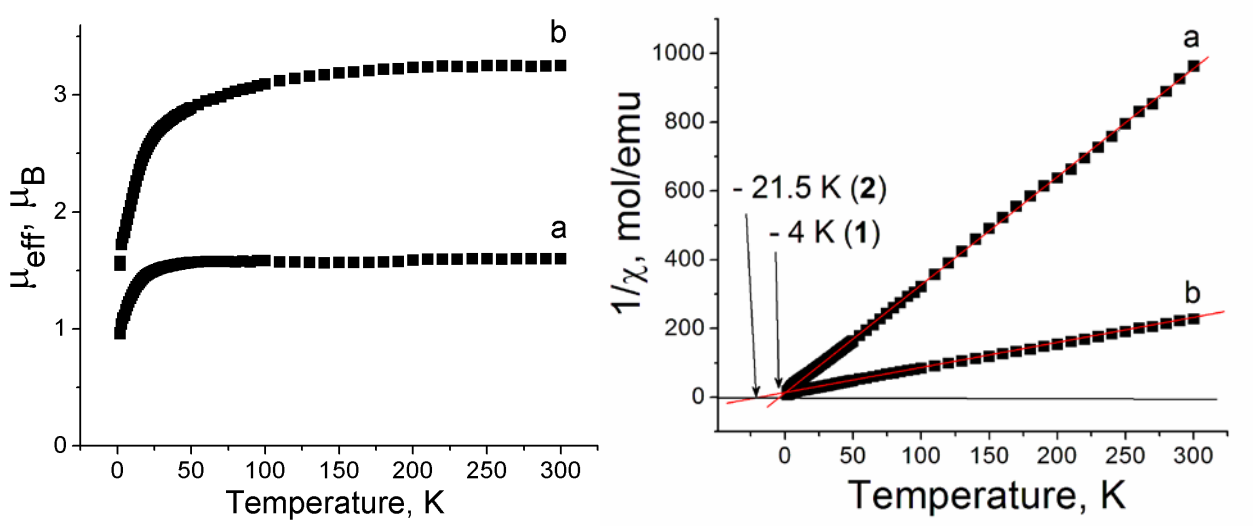

Figure 8. Temperature dependence of effective magnetic moment (left panel) and reciprocal molar magnetic susceptibility (right panel) for salts **1** (a) and **2** (b).

The magnetic properties of polycrystalline **1** and **2** were studied by EPR and SQUID techniques. Salt **1** shows an effective magnetic moment of 1.60 μ_B at 300 K (Fig. 8, left panel, curve a), which indicates a contribution of about one non-interacting S = 1/2 spin per formula unit (the temperature dependence of $\chi_M T$ is shown in Fig. S3a). Since the closed-shell diamagnetic F_8Pc^{4-} tetraanion is formed in accordance with optical spectra and theoretical calculations, the S = 1/2 spin can localize on Cu^{II}. The Weiss temperature of -4 K estimated in the 30–300 K range (Fig. 8, right panel, line a) indicates weak antiferromagnetic coupling between spins. This may be due to the large spatial separation between the Cu^{II} atoms (the shortest Cu···Cu distance is 8.58 Å).

The EPR spectrum of **1** supports the presence of S = 1/2 spins on the Cu^{II} atoms, since the salt manifests a strongly asymmetric signal (Fig. 9), which can be fitted by five components, with g_1

= 1.9634 and linewidth (ΔH) = 6.62 mT; g_2 = 2.0401 (ΔH = 7.83 mT); g_3 = 2.0892 (ΔH = 9.848 mT); g_4 = 2.1717 (ΔH = 16.93 mT); g_5 = 2.3500 (ΔH = 14.62 mT). The components with g_2 and g_4 have the highest integral intensity among the other components. All the observed components can be unambigously attributed to Cu^{II}, since the signal from the $Pc^{\bullet 3-}$ radical trianions is essentially narrower in the EPR spectrum of $[Cu^{II}(Pc)^{\bullet 3-}]^{\bullet -}$.[18] The main spectral feature can be explained as resulting from (1) the g-factor anisotropy with axially symmetric $g_{\parallel}$ and $g_{\perp}$ components and (2) the ^{63}Cu and ^{65}Cu hyperfine splittings (I = 3/2), although the additional hyperfine splitting by ^{14}N nuclei (I = 1) in the isoindole moiety was unfortunately not observed.[39]

Salt **2** manifests an effective magnetic moment of 3.25 μ_B at 300 K per formula unit (Fig. 7, left panel, curve b; the temperature dependence of $\chi_M T$ is shown in Fig. S3b). This value is close to the contribution of four non-interacting S = 1/2 spins (calculated value is μ_{eff} = 3.46 μ_B). These

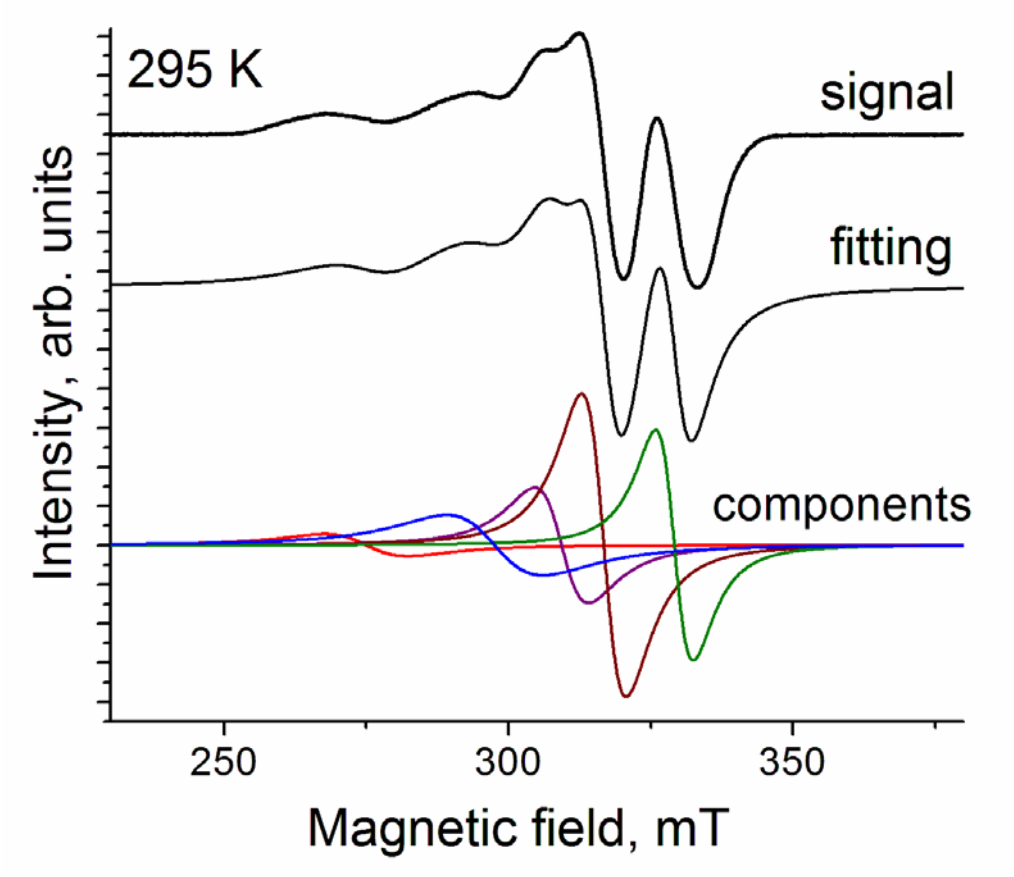

Figure 9. EPR spectrum of polycrystalline **1** at room temperature (295 K).

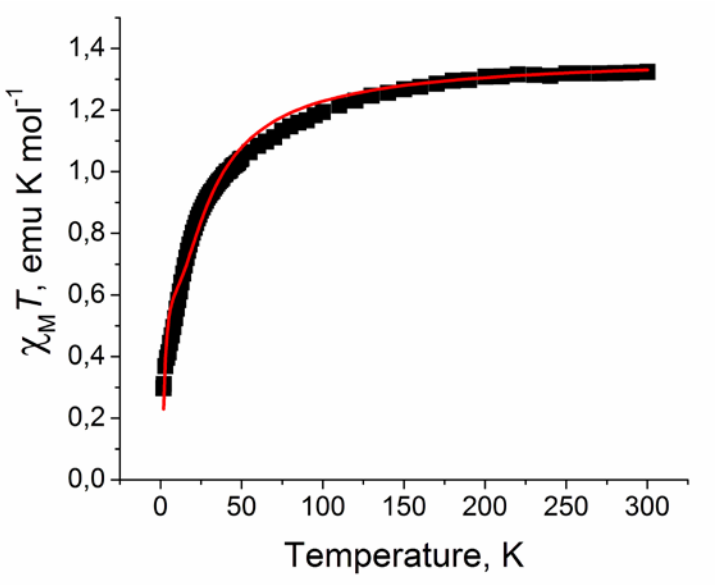

Figure 10. Temperature dependence of $\chi_M T$ (black squares) observed in **2** and approximation of the data by the Heisenberg model for four spin system[40] (red curve). See the text for parameters of fitting.

spins can originate from the $[Cu^{II}(F_{16}Pc)^{\bullet 3-}]^{\bullet -}$ radical anions of type II, which in accordance with theoretical calculations can have two S = 1/2 spins positioned on Cu^{II} and $F_{16}Pc^{\bullet 3-}$. In total, two $[Cu^{II}(F_{16}Pc)^{\bullet 3-}]^{\bullet -}$ radical anions per formula unit are present in **2** (the total number of S = 1/2 spins is four per formula unit). The formation of a diamagnetic $[Cu^{I}(F_{16}Pc)^{2-}]^{-}$ anion in **2**, with the different charge distribution, decreases the total magnetic moment of the salt in comparison with the case where only $[Cu^{II}(F_{16}Pc)^{\bullet 3-}]^{\bullet -}$ radical anions are present (in this case an effective magnetic moment of 4.24 μ_B is expected for six non-interacting S = 1/2 spins per formula unit). The Weiss temperature of −21.5 K estimated in the 80–300 K range (Fig. 8, right panel, line b) indicates antiferromagnetic coupling between spins.

To elucidate the magnetic interactions in the centrosymmetric $[Cu^{II}(F_{16}Pc)^{\bullet 3-}]_2$ (type II) dimers within the stacks separated by diamagnetic $[Cu^{I}(F_{16}Pc^{2-})]^{-}$ anions, we used the Heisenberg model for a four spin system, such as Cu(S_1)-J_2-F_{16}Pc(S_2)-J_1-F_{16}Pc(S_3)-J_2-Cu(S_4), where S_1, S_2, S_3, and S_4 are S = 1/2 spins. The fitting equation[40] is as follows:

$$\chi = f\frac{Ng^2\mu_B^2}{k_BT}\frac{10\exp(-E_1/k_BT)+2\exp(-E_2/k_BT)+2\exp(-E_3/k_BT)+2\exp(-E_4/k_BT)}{5\exp(-E_1/k_BT)+3\exp(-E_2/k_BT)+3\exp(-E_3/k_BT)+3\exp(-E_4/k_BT)+\exp(-E_5/k_BT)+\exp(-E_6/k_BT)}$$

$E_1 = -J_2 - J_1/2$

$E_2 = J_2 - J_1/2$

$E_3 = J_1/2 + (J_2^2 + J_1^2)^{1/2}$

$E_4 = J_1/2 - (J_2^2 + J_1^2)^{1/2}$

$E_5 = J_2 + J_1/2 + (4J_2^2 - 2J_2J_1 + J_1^2)^{1/2}$

$E_6 = J_2 + J_1/2 - (4J_2^2 - 2J_2J_1 + J_1^2)^{1/2}$

As a result, we obtained the antiferromagnetic interactions $J_1/k_B = -23.5$ K and $J_2/k_B = -8.1$ K under the conditions of $f = 0.9$ (fix) and $g = 2$ (fix) to reduce the number of parameters, indicating stronger intermolecular (J_1) and weaker intramolecular (J_2) magnetic interactions (Fig. 10). Under centrosymmetric conditions, it is also possible to model as F_{16}Pc(S_1)-J_2-Cu(S_2)-J_1-Cu(S_3)-J_2-F_{16}Pc(S_4), and also to obtain the intermolecular (J_1) and intramolecular (J_2) magnetic interactions. But the Cu(S_2)-Cu(S_3) direct magnetic interaction should not be strong, since the $d(x^2-y^2)$ orbital of Cu is directed not toward the paired Cu atom, but toward the F_{16}Pc plane.

Previously, it was also shown that the magnetic coupling between the paramagnetic central metal atoms and the $Pc^{\bullet 3-}$ radical trianions within one $[Cu^{II}(Pc)^{\bullet 3-}]^{\bullet -}$ (Cu^{II} ($S = 1/2$) and $Pc^{\bullet 3-}$ ($S = 1/2$)) or $[V^{IV}O(Pc)^{\bullet 3-}]^{\bullet -}$ unit (V^{IV} ($S = 1/2$) and $Pc^{\bullet 3-}$ ($S = 1/2$)) is antiferromagnetic and weak, since the Weiss temperatures for the salts with these isolated units are only –4 and –9.6 K, respectively.[18] Therefore, the magnetic properties of this salt are mainly dominated by the coupling between $(F_{16}Pc)^{\bullet 3-}$ macrocycles in the dimers. This coupling is relatively weak in comparison with that in the $[Ti^{IV}O(Pc)^{\bullet 3-}]_2$ dimers in $(Et_4N^+)[Ti^{IV}O(Pc)^{\bullet 3-}]\cdot C_6H_4Cl_2$, in which short interplanar distances (3.129 Å) and larger overlap integrals result in a diamagnetic state, even below 150 K.[18] The reason for the weaker intermolecular magnetic interaction may be attributable to the larger interplanar F_{16}Pc distance in the dimers of 3.275 Å and smaller overlap integrals between them. EPR signals are not manifested in the spectrum of **2** at room temperature.

A similar situation is observed for the π-stacking compounds with the $[Fe^{I}(Cl_{16}Pc)^{2-}]^{-}$ anions containing paramagnetic Fe^{I} centers (S = 1/2).[20] Observation of the EPR spectrum for Fe^{I} is only possible in the salt with isolated $[Fe^{I}(Cl_{16}Pc)^{2-}]^{-}$ anions only.[21]

Conclusion

Two new salts of copper octafluoro- and hexadecafluorophthalocyanines have been obtained in crystalline form. Salt **1** contains dianions, in which two extra electrons are delocalized over the F_8Pc macrocycle, and the charged state of Cu^{II} remains unchanged. Salt **2** is the first example of a π-stacking compound containing metal phthalocyanine with the $F_{16}Pc^{\bullet 3-}$ radical trianions. The unusual charge distibution, in which metal-reduced and macrocycle-reduced anions are stacked to form a $\cdots[Cu^{II}(F_{16}Pc)^{\bullet 3-}]^{\bullet -}\cdots[Cu^{I}(F_{16}Pc)^{2-}]^{-}\cdots[Cu^{II}(F_{16}Pc)^{\bullet 3-}]^{\bullet -}\cdots$ arrangement, proves the internal degree of freedom of the charge distibution within a molecule, whether the extra electron is accomodated on the metal center or on the Pc macrocycle. We believe that hexadecafluoro- or hexadecachlorophthalocyanines of other metals can show a more homogeneous charge distribution, allowing exotic materials to be synthesized.

Supporting Information: The IR spectra of starting compounds and salts **1** and **2**, and details of the DFT calculations for **1** and **2** are available free of charge via the Internet at http://pubs.acs.org.

Author Information

Corresponding Author

*E-mail for D.V.K.: konarev@icp.ac.ru.

Acknowledgment

The work was supported by RFBR grant № 16-33-00588 and JSPS KAKENHI Grant Numbers 15K17901, 23225005, and 26288035. Theoretical calculations were performed at the Research Center for Computational Science, Okazaki, Japan, and under Collaborative Research Program for Young Scientists at Academic Center for Computing and Media Studies, Kyoto University.

References

1. Petersen, J. L.; Schramm, C. S.; Stojakovic, D. R.; Hoffman, B. M.; Marks, T. J. A new class of highly conductive molecular solids: the partially oxidized phthalocyanines. *J. Am. Chem. Soc*. **1977**, *99*, 286-288.
2. Inabe, T.; Tajima, H. Phthalocyanines - versatile components of molecular conductors. *Chem. Rev*. **2004**, *104*, 5503-5534.
3. Hasegawa, H.; Naito, T.; Inabe, T.; Akutagawa, T.; Nakamura, T. A highly conducting partially oxidized salt of axially substituted phthalocyanine. Structure and physical properties of TPP[Co(Pc)$(CN)_2]_2$ {TPP=tetraphenylphosphonium, [Co(Pc)$(CN)_2$]= dicyano(phthalocyaninato)cobalt(III)}. *J. Mater. Chem*. **1998**, *8*, 1567-1570.
4. Matsuda, M.; Naito, T.; Inabe, T.; Hanasaki, N.; Tajima, H.; Otsuka, T.; Awaga, K.; Narymbetov, B.; Kobayashi, H. *J.* A one-dimensional macrocyclic π-ligandconductor carrying a magnetic center. Structure and electrical, optical and magnetic properties of TPP[Fe(Pc)$(CN)_2]_2$ {TPP = tetraphenylphosphonium and [Fe(Pc)$(CN)_2$] = dicyano(phthalocyaninato)iron(III)}. *Mater. Chem*. **2000**, *10*, 631-636.
5. Matsuda, M.; Naito, T.; Inabe, T.; Hanasaki, N.; Tajima, H. Structure and electrical and magnetic properties of $(PTMA)_x$[M(Pc)$(CN)_2$]· *y*(solvent) (PTMA = phenyltrimethylammonium and [M(Pc)$(CN)_2$] = dicyano(phthalocyaninato)M^{III} with M = Co and Fe). Partial oxidation by partialsolvent occupation of the cationic site. *J. Mater. Chem*. **2001**, *11*, 2493- 2497.
6. Miller, J. S.; Vazquez, C.; Calabrese, J. C.; McLean, M. L.; Epstein, A. J Cooperative magnetic behavior of α- and β-manganese(III) phthalocyanine tetracyanoethenide (1:1), $[Mn^{III}Pc]^{+}\cdot[TCNE]^{\bullet-}$. *Adv. Mater*. **1994**, *6*, 217-221.
7. Rittenberg, D. K. ; Baars-Hibbe, L.; Böhm, A. B.; Miller, J. S. Manganese(II) octabutoxynaphthalocyanine and its ferrimagnetic electron-transfer salt with TCNE. *J. Mater. Chem*. **2000**, *10*, 241-244.
8. Tosatti, E.; Fabrizio, M.; Tóbik, J.; Santoro, G. E. Strong correlations in electron doped

phthalocyanine conductors near half filling. *Phys. Rev. Lett*., **2004**, *93*, 117002.

9. Konarev, D. V.; Zorina, L. V.; Khasanov, S. S.; Hakimova, E. U.; Lyubovskaya, R. N. Structure and magnetic properties of ionic compound $(Cp^*_2Cr^+)\cdot(Fe^IPc^-)\cdot(C_6H_4Cl_2)_4$ containing negatively charged iron phthalocyanine. *New J. Chem*. **2012**, *36*, 48-51.
10. Cissell, J. A.; Vaid, T. P.; Rheingold, A. L. Aluminum tetraphenylporphyrin and aluminum phthalocyanine neutral radicals. *Inorg. Chem.* **2006**, *45*, 2367–2369.
11. Wong, E. W. Y.; Walsby, C. J.; Storr, T.; Leznoff, D. B. Phthalocyanine as a chemically inert, redox-active ligand: structural and electronic properties of a Nb(IV)-oxo complex incorporating a highly reduced phthalocyanine(4−) anion, *Inorg. Chem.* **2010**, *49*, 3343–3350.
12. Wong, E. W. Y.; Leznoff, D. B. Synthesis and structural characterization of a magnesium phthalocyanine(3–) anion. *J. Porph. Phth.* **2012**, *16*, 154–162.
13. Konarev, D. V.; Khasanov, S. S.; Ishikawa, M.; Otsuka, A.; Yamochi, H.; Saito, G.; Lyubovskaya, R. N. Structure and magnetic properties of ternary $(Me_4P^+)\cdot\{[Fe^IPc(-2)]^-\}\cdot$TPC and $(Me_4P^+)\cdot\{[Fe^IPc(-2)]^-\}\cdot(TBPDA)_{0.5}$ complexes with one- and two-dimensional packing of iron(I) phthalocyanine anions. *Inorg. Chem*. **2013**, *52*, 3851-3859.
14. Konarev, D. V.; Kuzmin, A. V.; Khasanov, S. S.; Lyubovskaya, R. N. Zwitterionic $\{Fe(I)Pc(-2)^-\}\cdot(TMP^+)$ assemblies comprising anionic iron(I) phthalocyanines and coordinating *N*,*N*,*N*`-trimethylpiperazinium cations. *Dalton Trans*. **2013**, *42*, 9870 - 9876.
15. Konarev, D. V.; Kuzmin, A. V.; Simonov, S. V.; Khasanov, S. S.; Otsuka, A.; Yamochi, H.; Saito, G.; Lyubovskaya, R. N. Ionic compound containing iron phthalocyanine $(Fe^IPc)^-$ anions and the $(C_{70}^-)_2$ dimers. Optical and magnetic properties of $(Fe^IPc)^-$ in solid state. *Dalton Trans*. **2012**, *41*, 13841-13847.
16. Konarev, D. V.; Zorina, L. V.; Khasanov, S. S.; Litvinov, A. L.; Otsuka, A.; Yamochi, H.; Saito, G.; Lyubovskaya, R. N. Molecular structure, optical and magnetic properties of metal-

free phthalocyanine radical anions in crystalline salts $(H_2Pc^{\bullet-})$(cryptand[2,2,2][Na^+])·1.5$C_6H_4Cl_2$ and $(H_2Pc^{\bullet-})(TOA^+)\cdot C_6H_4Cl_2$ (TOA^+ is tetraoctylammonium cation). *Dalton Trans.* **2013**, *42*, 6810-6816.

17. Konarev, D. V.; Kuzmin, A. V.; Khasanov, S. S.; Otsuka, A.; Yamochi, H.; Saito, G.; Lyubovskaya, R. N. Design, crystal structures and magnetic properties of anionic salts containing fullerene C_{60} and indium(III) bromine phthalocyanine radical anions. *Dalton Trans*. **2014**, *43*, 13061-13069.
18. Konarev, D. V.; Kuzmin, A. V.; Faraonov, M. A.; Ishikawa, M.; Nakano, Y., Khasanov, S. S.; Otsuka, A.; Yamochi, H.; Saito, G.; Lyubovskaya, R. N. Synthesis, crystal structures, optical and magnetic properties of crystalline salts with radical anions of metal-containing and metal-free phthalocyanines. *Chem. Eur. J.*, **2015**, *21*, 1014-1028.
19. Konarev, D. V. ; Troyanov, S. I.; Ishikawa, M.; Faraonov, M. A.; Otsuka, A.; Yamochi, H.; Saito, G.; Lyubovskaya, R. N. Molecular structure, optical and magnetic properties of the $\{Sn^{IV}Cl_2Pc(3-)\}^{\bullet-}$ radical anions containing negatively charged Pc ligands. *J. Porph. Phth*. **2014**, *18*, 1157-1163.
20. Konarev, D. V.; Zorina, L. V.; Ishikawa, M.; Khasanov, S. S.; Otsuka, A.; Yamochi, H.; Saito, G.; Lyubovskaya, R. N. Molecular design of anionic phthalocyanines with π-π stacking columnar arrangement. Crystal structures, optical and magnetic properties of salts with the iron(I) hexadecachlorophthalocyanine anions. *Cryst. Groth Des*. **2013**, *13*, 4930−4939.
21. Konarev, D. V.; Kuzmin, A. V.; Ishikawa, M.; Nakano, Y.; Faraonov, M. A.; Khasanov, S. S.; Otsuka, A.; Yamochi, H.; Saito, G.; Lyubovskaya, R. N. Layered salts with iron hexadecachlorophthalocyanine anions. The formation of $[\{FeCl_{16}Pc\}_2]^{3-}$ dimers containing $[Fe^{I}Cl_{16}Pc(2-)]^-$ and diamagnetic $[Fe^{0}Cl_{16}Pc(2-)]^{2-}$ anions. *Eur. J. Inorg. Chem.* **2014**, 3863-3870.
22. Konarev, D. V.; Khasanov, S. S.; Yudanova, E. I.; Lyubovskaya, R. N. The η^2-complex of

nickel bis(diphenylphosphino)propane with fullerene: (Ni(dppp)·(η^2-C_{60})·(solvent) obtained by reduction. *Eur. J. Inorg. Chem.* **2011**, 816-820.

23. Bruker Analytical X-ray Systems, Madison, Wisconsin, U.S.A, **1999.**
24. Sheldrick, G. M. A short history of SHELX. *Acta Crystallogr., Sect. A: Fundam. Crystallogr.* **2008**, *64*, 112-122.
25. Peverati, R.; Truhlar, D. G. Improving the accuracy of hybrid meta-GGA density functionals by range separation. *J. Phys. Chem. Lett.*, **2011**, *2*, 2810-2817.
26. a). Peterson, K. A.; Puzzarini, C. Systematically convergent basis sets for transition metals. II. Pseudopotential-based correlation consistent basis sets for the group 11 (Cu, Ag, Au) and 12 (Zn, Cd, Hg) elements. *Theor. Chem. Acc.*, **2005**, *114*, 283-296; b). Feller, D. The role of databases in support of computational chemistry calculations. *J. Comp. Chem.*, **1996**, *17*, 1571-1586; c). Schuchardt, K. L.; Didier, B. T.; Elsethagen, T.; Sun, L.; Gurumoorthi, V.; Chase, J.; Li, J.; Windus, T. L., Basis Set Exchange: A Community Database for Computational Sciences. *J. Chem. Inf. Model*., **2007**, *47*, 1045-1052.
27. Dunning, Jr., T. H. Gaussian basis sets for use in correlated molecular calculations. I. The atoms boron through neon and hydrogen. *J. Chem. Phys.*, **1989**, *90*, 1007-1023.
28. NBO Version 3.1, Glendening, E. D.; Reed, A. E.; Carpenter, J. E.; Weinhold F.
29. Gaussian 09, Revision D.01, Frisch, M. J.; Trucks, G. W.; Schlegel, H. B.; Scuseria, G. E.; Robb, M. A.; Cheeseman, J. R.; Scalmani, G.; Barone, V.; Mennucci, B.; Petersson, G. A.; Nakatsuji, H.; Caricato, M.; Li, X.; Hratchian, H. P.; Izmaylov, A. F.; Bloino, J.; Zheng, G.; Sonnenberg, J. L.; Hada, M.; Ehara, M.; Toyota, K.; Fukuda, R.; Hasegawa, J.; Ishida, M.; Nakajima, T.; Honda, Y.; Kitao, O.; Nakai, H.; Vreven, T.; Montgomery, Jr. J. A.; Peralta, J. E.; Ogliaro, F.; Bearpark, M.; Heyd, J. J.; Brothers, E.; Kudin, K. N.; Staroverov, V. N.; Kobayashi, R.; Normand, J.; Raghavachari, K.; Rendell, A.; Burant, J. C.; Iyengar, S. S.; Tomasi, J.; Cossi, M.; Rega, N.; Millam, J. M.; Klene, M.; Knox, J. E.; Cross, J. B.; Bakken, V.; Adamo, C.; Jaramillo, J.; Gomperts, R.; Stratmann, R. E.; Yazyev, O.; Austin, A. J.;

Cammi, R.; Pomelli, C.; Ochterski, J. W.; Martin, R. L.; Morokuma, K.; Zakrzewski, V. G.; Voth, G. A.; Salvador, P.; Dannenberg, J. J.; Dapprich, S.; Daniels, A. D.; Farkas, Ö.; Foresman, J. B.; Ortiz, J. V.; Cioslowski, J.; Fox, D. J. Gaussian, Inc., Wallingford CT, **2009**.

30. a). Keizer, S. P.; Mack, J.; Bench, B. A.; Gorun, S. M.; Stillman, M. J., Spectroscopy and electronic structure of electron deficient zinc phthalocyanines. *J. Am. Chem. Soc*., **2003**, *125*, 7067–7085; b). Moons, H.; Łapok, Ł.; Loas, A.; Van Doorslaer, S.; Gorun, S. M. Synthesis, X-ray structure, magnetic resonance, and DFT analysis of a soluble copper(II) phthalocyanine lacking C−H bonds, *Inorg. Chem.*, **2010**, *49*, 8779–8789; c). Moons, H.; Loas, A.; Gorun, S.M.; Van Doorslaer , S. Photoreduction and light-induced triplet-state formation in a single-site fluoroalkylated zinc phthalocyanine, *Dalton Trans*., **2014**, *43*, 14942-14948.

31. Cissell, J. A.; Vaid, T. P.; DiPasquale, A. G.; Rheingold, A. L., Germanium phthalocyanine, GePc, and the reduced complexes SiPc(pyridine)$_2$ and GePc(pyridine)$_2$ containing antiaromatic π-electron circuits. *Inorg. Chem*. **2007**, *46*, 7713-7715.

32. Zhou, W.; Platel, R. H.; Tasso, T. T.; Furuyama, T.; Kobayashi, N.; Leznoff, D. B. Reducing zirconium(IV) phthalocyanines and the structure of a $Pc^{4-}Zr$ complex. *Dalton Trans.*, **2015**, *44*, 13955-13961.

33. Konarev, D. V.; Kuzmin, A. V.; Nakano, Y.; Faraonov, M. A.; Khasanov, S. S.; Otsuka, A. Yamochi, H.; Saito, G.; Lyubovskaya, R. N. Coordination complexes of transition metals (M = Mo, Fe, Rh and Ru) with tin(II) phthalocyanine in neutral, radical anion and dianionic states. *Inorg. Chem.*, **2016**, *55*, 1390–1402.

34. Hoshino, A.; Takenaka Y.; Miyaji, H. Redetermination of the crystal structure of α-copper phthalocyanine grown on KCl. *Acta Crystallogr. Sect. B: Struct. Sci*. **2003**, *59*, 393- 403.

35. (a) Whangbo, M.-H.; Hoffmann, R. The band structure of the tetracyanoplatinate chain. *J. Am. Chem. Soc.*, **1978**, *100*, 6093-6098; (b) Ren, J.; Liang, W.; Whangbo, M.-H. Crystal and electronic structure analysis using CAESAR **1998**, Prime Color Software, Inc. (this book can be downloaded free of charge from the website: http://www.PrimeC.com/). Default parameters were used.

36. Takano, S.; Naito, T.; Inabe, T. Ladder-type phthalocyanine conductor, [PXX][Co(Pc)$(CN)_2$] (PXX = perixanthenoxanthene, Co(Pc)$(CN)_2$ = dicyano(phthalocyaninato)cobalt(III)). *Chem. Lett*. **1998**, *27*, 1249-1250.

37. Matsuda, M.; Asari, T.; Naito, T.; Inabe, T.; Hanasaki, N.; Tajima, H. Structure and physical properties of low-dimensional molecular conductors. [PXX][Fe^{III}(Pc)$(CN)_2$] and [PXX][Co^{III}(Pc)$(CN)_2$] (PXX =*peri*-xanthenoxanthene, Pc = phthalocyaninato). *Bull. Chem. Soc. Jpn*. **2003**, *76*, 1935-1940.

38. Asari, T.; Naito, T.; Inabe, T.; Matsuda, M.; Tajima, H. Novel phthalocyanine conductor containing two-dimensional Pc stacks. [PXX]$_2$[Co(Pc)$(CN)_2$] (PXX = *peri*-xanthenoxanthene, Co(Pc)$(CN)_2$ = dicyano(phthalocyaninato)cobalt(III)). *Chem. Lett*. **2004**, *33*, 128-129.

39. (a) Moons, H.; Łapok, Ł.; Loas, A.; Van Doorslaer, S., M. Gorun, S. Synthesis, X-ray structure, magnetic resonance, and DFT analysis of a soluble copper(II) phthalocyanine lacking C-H bonds. *Inorg. Chem*., **2010**, *49*, 8779-8789; (b) Matrix effects on copper(II)phthalocyanine complexes. A combined continuous wave and pulse EPR and DFT study. Finazzo, C.; Calle, C.; Stoll, S.; Van Doorslaer, S.; Schweigery, A. *Phys. Chem. Chem. Phys.*, **2006**, *8*, 1942–1953; (c) Creiner, S. P.; Rowlands, D. L.; Kreilick, R. W. EPR and ENDOR study of selected porphyrin- and phthalocyanine-copper complexes. *J. Phys. Chem.* **1992**, *96*, 9132-9139.

40. Liu, Z.-L.; Li-Cun , Liao, D.-Z.; Jiang , Z.-H.; Yan. S.-P. Oxamido-bridged bimetallic complexes involving nitronyl nitroxide radical ligands: crystal structure and magnetic

behavior. *Cryst. Grow. Des*., **2005**, *5*, 783-787.

SYNOPSYS

Crystalline anionic salts with copper octafluoro- and hexadecafluorophthalocyanines have been obtained: $(Bu_4N^+)_2[Cu^{II}(F_8Pc)^{4-}]^{2-}\cdot 2C_6H_4Cl_2$ (**1**) and $(PPN^+)_3[Cu(F_{16}Pc)]_3^{3-}\cdot 2C_6H_5CN$ (**2**). Closed-shell F_8Pc^{4-} tetraanions are formed in **1** without reduction of Cu^{II}. Salt **2** contains π-π stacks of $\cdots[Cu^{II}(F_{16}Pc)^{\bullet 3-}]^{\bullet -}\cdots[Cu^{I}(F_{16}Pc)^{2-}]^{-}\cdots[Cu^{II}(F_{16}Pc)^{\bullet 3-}]^{\bullet -}\cdots$, suggested by DFT calculations based on the crystal structure and supported by the observed magnetism.

For Table of Contents Only